

Energy Transfer and Exciplex Formation and Their Impact on Exciton and Charge Carrier Dynamics in Organic Films

Whitney E. B. Shepherd,[†] Andrew D. Platt,[†] Mark J. Kendrick,[†] Marsha A. Loth,[‡] John E. Anthony,[‡] and Oksana Ostroverkhova^{*,†}

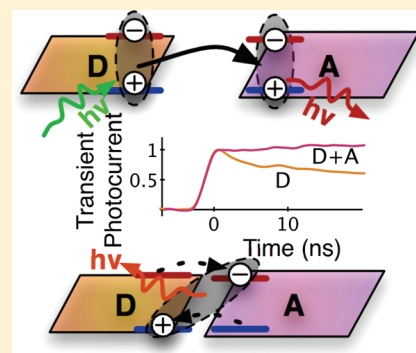
[†]Department of Physics, Oregon State University, Corvallis, Oregon 97331, United States

[‡]Department of Chemistry, University of Kentucky, Lexington, Kentucky 40506, United States

S Supporting Information

ABSTRACT: We report Förster resonant energy transfer (FRET) with a Förster radius R_0 of 4.8 nm and exciplex formation in composites containing two functionalized anthradithiophene (ADT) derivatives, ADT-TES-F (donor, D) and ADT-TIPS-CN (acceptor, A) depending on the D–A distance. In composites containing bulk D/A heterojunctions, exciplex photoluminescence (PL) emission peaked at ~ 668 nm dominated the PL spectra. The exciplex contributed to charge carrier photogeneration on nanosecond time scales in composites, in contrast to sub-500 ps carrier photogeneration observed in ADT-TES-F pristine films. Finally, significantly slower charge carrier recombination was obtained in composites, as compared to that of pristine ADT-TES-F films, due to electron trapping at the ADT-TIPS-CN enabling the hole to propagate in the ADT-TES-F host.

SECTION: Electron Transport, Optical and Electronic Devices, Hard Matter



Organic optoelectronic materials have shown promise in a wide range of applications, from display technologies to photovoltaics.¹ Solution-processable materials, additionally, can be readily combined in composite systems, which can drastically alter the optical and electronic properties.² Organic bulk heterojunctions have been utilized in solar cells,³ photorefractive devices,⁴ and photodetectors⁵ due to enhanced charge carrier photogeneration occurring as a result of photoinduced electron transfer between the donor (D) and acceptor (A) molecules. A competing process, energy transfer (such as Förster resonant energy transfer (FRET)), which also occurs in D/A systems, has been exploited in solar cells to improve light harvesting⁶ and in organic light-emitting diodes (OLEDs) to enhance emission efficiency and to control emission wavelength.⁷ In the case of D/A systems with the energy level offsets between the D and A of only a few tenths of an eV, exciplex states may form.⁸ Exciplexes are a transient species consisting of a D/A complex involving the excited state of the D (A) and the ground state of the A (D) and are characterized by long radiative decay times and red-shifted photoluminescence (PL) spectra.^{9,10} The formation of exciplexes is well-documented in a variety of polymer and small-molecular-weight blends.^{11–14} Recently, exciplexes generated significant interest due to their role in charge photogeneration and recombination in solar cells^{8,15,16} and in broad-band emission in OLEDs.^{17,18}

The fluorinated anthradithiophene (ADT) derivative functionalized with triethylsilylethynyl (TES) side groups, ADT-TES-F (inset of Figure 1), exhibits charge carrier mobilities of

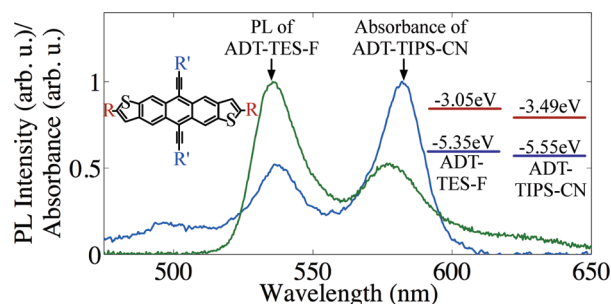


Figure 1. Normalized absorbance of ADT-TIPS-CN and PL of ADT-TES-F in dilute toluene solution. Structures of the two molecules as well as their HOMO/LUMO levels are also shown. ADT-TES-F: R = F, R' = TES. ADT-TIPS-CN: R = CN, R' = triisopropylsilylethynyl (TIPS).

$>1.5 \text{ cm}^2/(\text{V s})$, high photoconductivity, and strong PL in solution-deposited films.^{19–22} The addition of a different ADT derivative, ADT-TIPS-CN (inset of Figure 1), as a guest into a host of ADT-TES-F has been shown to have dramatic effects on transient photocurrent dynamics and PL spectra, indicative of photoexcited charge- and/or energy-transfer processes between ADT-TES-F (D) and ADT-TIPS-CN (A).² However, the exact nature of these processes has not yet been established. The complexity of the interactions present in the ADT-TES-F/ADT-TIPS-CN

Received: December 17, 2010

Accepted: January 24, 2011

composites, which includes aggregation of both donor and acceptor molecules,²³ FRET due to a strong overlap of the donor emission and acceptor absorption spectra (Figure 1), and possible exciplex formation due to relatively small offsets in the donor and acceptor energy levels (inset of Figure 1), makes them an interesting model system for exploring effects of various D/A interactions on exciton and charge carrier dynamics. In this Letter, we establish conditions for FRET and exciplex formation in ADT-TES-F/ADT-TIPS-CN systems and their contributions to (opto)electronic properties of ADT-TES-F/ADT-TIPS-CN-based thin films. Because D and A molecules used in our studies are structurally similar, as opposed to typical D/A pairs used in organic bulk heterojunction solar cells, ADT-TES-F/ADT-TIPS-CN systems could represent a starting point for design of functionalized D and A molecules with controlled HOMO–LUMO levels and molecular packing.

In order to separately study the FRET and exciplex formation processes, we prepared spin-coated thin films of the following: (1) a mixture of equal parts (50/50) of ADT-TES-F and ADT-TIPS-CN added in various concentrations to a PMMA matrix and (2) composites containing ADT-TIPS-CN added to ADT-TES-F in various concentrations. Samples in PMMA were prepared at total ADT-TES-F and ADT-TIPS-CN concentrations ranging from 4.9×10^{-4} to 5.9×10^{-2} M and are denoted as $P(c)$, where c is the concentration of the ADT-TES-F/ADT-TIPS-CN mixture per PMMA in molarity. The average spacings between the ADT-TES-F and ADT-TIPS-CN molecules as calculated from concentrations are listed in Table S1 of the Supporting Information. Composite samples (ADT-TIPS-CN guest molecules in the ADT-TES-F host) were prepared at concentrations of 1.8×10^{-4} M to 1.8×10^{-1} M and are denoted as $C(c)$ where c is the concentration of ADT-TIPS-CN per ADT-TES-F in molarity. Samples of ADT-TES-F alone in PMMA, as well as pristine ADT-TES-F and ADT-TIPS-CN films, were also prepared as controls.

ADT-TES-F/ADT-TIPS-CN in PMMA. PL spectra from ADT-TES-F (D) and ADT-TIPS-CN (A) embedded in a PMMA host are shown in Figure 2a. The inset of Figure 2a shows an expanded view of the donor emission. As the ADT-TES-F/ADT-TIPS-CN concentration increased, corresponding to a smaller D–A distance, the donor emission was quenched, while that of the acceptor increased, which suggests FRET. Multiplex fitting (e.g., Figure S1 in the Supporting Information and ref 24) showed that in all but the most concentrated sample, $P(5.9 \times 10^{-2})$, only PL emissions from isolated donor and acceptor molecules were present, and no aggregation effects were observed. The FRET radius for energy transfer from the isolated ADT-TES-F donor to the isolated ADT-TIPS-CN acceptor was calculated (as detailed in Supporting Information) using spectra in Figure 1 to be $R_0 = 4.8$ nm (which would correspond to a concentration, c , of 2.8×10^{-2} M), consistent with the trends exhibited by PL data in Figure 2. In $P(5.9 \times 10^{-2})$, additional spectral features appeared at above ~ 640 nm, attributed to the donor and acceptor aggregate emission. This emission is broadened and red-shifted with respect to that of the isolated donor and acceptor molecules. This is consistent with previous work on aggregation of ADT derivatives in a PMMA host, which show a strong onset of aggregate effects at this concentration.²³ Changes in the PL spectra were accompanied by changes in PL lifetimes. At low concentrations of ADT-TES-F/ADT-TIPS-CN in PMMA (large D–A distances), decays of the donor emission were single-exponential, with the donor lifetime approaching that of isolated

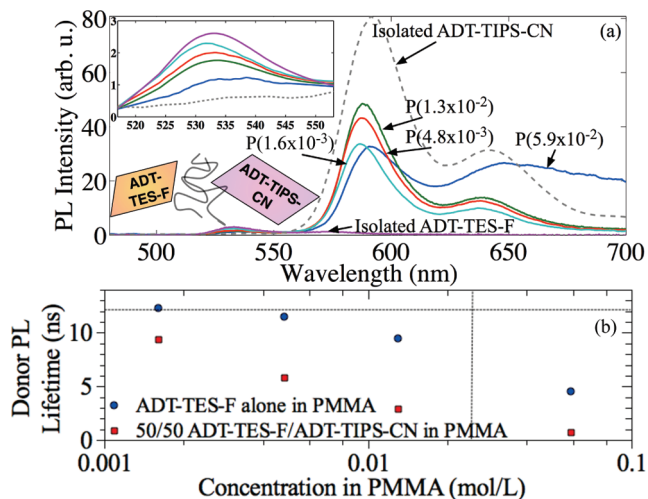


Figure 2. (a) PL spectra of 50/50 mixtures of ADT-TES-F (D) and ADT-TIPS-CN (A) in PMMA films, normalized at 577 nm to illustrate energy transfer. The inset shows a decrease in the donor PL as the concentration of ADT-TIPS-CN increases due to FRET. (b) Weighted average of PL lifetimes of the donor in PMMA films as a function of total concentration c in D/A and in donor-only PMMA films. A lifetime of 12.1 ns, which corresponds to the isolated donor molecules in PMMA, is indicated. The vertical line marks the concentration corresponding to the calculated FRET radius R_0 of 4.8 nm.

ADT-TES-F in PMMA, which is ~ 12.1 ns (Figure 2b).^{22,23} As the concentration increased, the donor PL decay became faster due to FRET²⁵ and, at higher concentrations, biexponential and yet faster due to aggregate effects.²³ For samples exhibiting biexponential decays, $P(5.9 \times 10^{-2})$ and $P(1.3 \times 10^{-2})$, the weighted average of the two lifetimes obtained from biexponential fits was plotted in Figure 2b. As seen from the figure, which also includes lifetimes from ADT-TES-F alone in PMMA, shortening of the lifetimes due to aggregation effects had a considerably weaker concentration dependence as compared to that due to FRET. For example, in $P(5.9 \times 10^{-2})$, the lifetime of the ADT-TES-F donor in the ADT-TES-F/ADT-TIPS-CN/PMMA system was a factor of ~ 6 shorter than that of the ADT-TES-F alone at the same concentration in PMMA.

ADT-TIPS-CN (Guest) in ADT-TES-F (Host) Composite Films. In these samples, the ADT-TES-F and ADT-TIPS-CN molecules are in direct contact with each other, forming D/A interfaces. Figure 3 shows PL spectra obtained under 355 nm excitation from composite samples $C(3.6 \times 10^{-4})$, $C(3.6 \times 10^{-3})$, and $C(3.6 \times 10^{-2})$ as well as those from pristine films of ADT-TES-F and ADT-TIPS-CN. Upon addition of the ADT-TIPS-CN to ADT-TES-F, the ADT-TES-F emission was strongly suppressed. At an ADT-TIPS-CN concentration of 3.6×10^{-4} M, multiplex fitting of the PL spectrum revealed that only $\sim 32\%$ of the total emission was from ADT-TES-F aggregates (similar to those in pristine ADT-TES-F films; see Table S2 (Supporting Information) for a PL spectral peak catalogue).^{23,24} The remaining $\sim 68\%$ was due to a new band, centered at ~ 668 nm, which could not be accounted for from either aggregate or isolated molecule spectra of either species. Upon increase in the ADT-TIPS-CN concentration, the ~ 668 nm peak (which corresponds to an energy of 1.86 eV) continued to dominate the total PL emission of the composite samples, accounting for ~ 59 and 55% of the emission in the $C(3.6 \times 10^{-3})$ and $C(3.6 \times 10^{-2})$ samples, respectively. The remaining ~ 41 and 45% of the

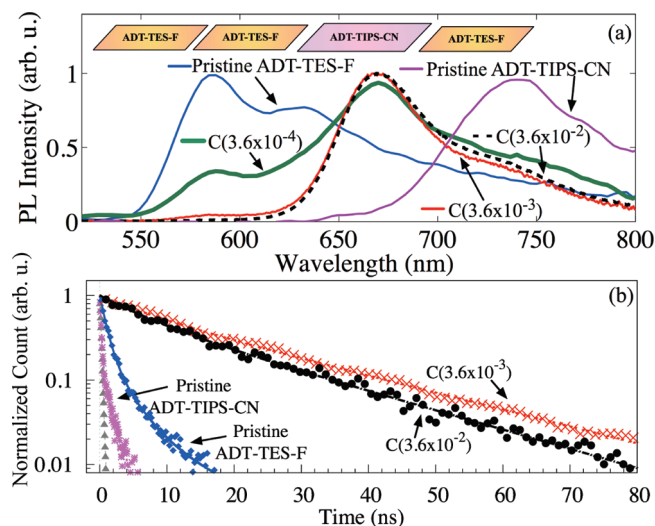


Figure 3. (a) PL spectra of ADT-TES-F/ADT-TIPS-CN composite films with varying concentrations of ADT-TIPS-CN. (b) Normalized PL decays measured in the composite films. The instrument response function (IRF) is also shown. PL spectra and decays of pristine ADT-TES-F and ADT-TIPS-CN films are included.

total emission in these samples originated from ADT-TIPS-CN aggregates (Table S2, Supporting Information). The energy of 1.86 eV matches the difference between the HOMO level of ADT-TES-F and the LUMO level of ADT-TIPS-CN (inset of Figure 1). Absorption spectra from samples with ADT-TIPS-CN concentrations of up to 1.8×10^{-1} M showed only additive contributions from ADT-TES-F and ADT-TIPS-CN pristine film behaviors, suggesting that the complex which emits at 668 nm is an excited-state species, in particular, an exciplex formed between ADT-TES-F in the ground state and photoexcited ADT-TIPS-CN. Observation of dominant exciplex emission in the composite samples under 532 and 633 nm illumination, which predominantly excited the ADT-TES-F and ADT-TIPS-CN, respectively, indicates that the exciplex can be formed through the excitation of either the donor or the acceptor. PL lifetimes measured in composite samples shown in Figure 3b exhibit the emergence of a ~ 19 – 22 ns lifetime upon addition of the ADT-TIPS-CN to ADT-TES-F. This is longer than the PL lifetimes for either ADT-TES-F (aggregate: ~ 2 – 3 ns; isolated molecule: ~ 10 – 13 ns)²³ or ADT-TIPS-CN (aggregate: ~ 0.2 – 1.7 ns; isolated molecule: ~ 13 – 16 ns),²² which confirms exciplex formation in these composites.²⁶

In order to establish effects of exciplex formation on photoexcited charge carrier dynamics, we measured photocurrents under pulsed and continuous wave (cw) photoexcitation in the composite films (refer to Supporting Information for experimental methods). Transient photocurrents (I_{ph}) obtained in pristine ADT-TES-F, $C(3.6 \times 10^{-3})$, and $C(3.6 \times 10^{-2})$ films upon 355 nm, $1 \mu\text{J}/\text{cm}^2$, 500 ps pulsed excitation at the applied electric field of 1.2×10^5 V/cm are shown in Figure 4.

In pristine ADT-TES-F films, fast (sub-500 ps, limited by the laser pulse width) charge carrier photogeneration was observed, consistent with previous studies.^{2,21,22} The peak amplitude (at $t = 0$ in Figure 4) was $\sim 40 \mu\text{A}$. After a fast initial decay of the photocurrent, a slow component due to dispersive transport, described by a power-law function $I_{ph} \sim t^{-\beta}$ (with $\beta = 0.16$ in the film in Figure 4), persisted to at least microsecond time scales. In the composite samples $C(3.6 \times 10^{-3})$ and $C(3.6 \times 10^{-2})$, in

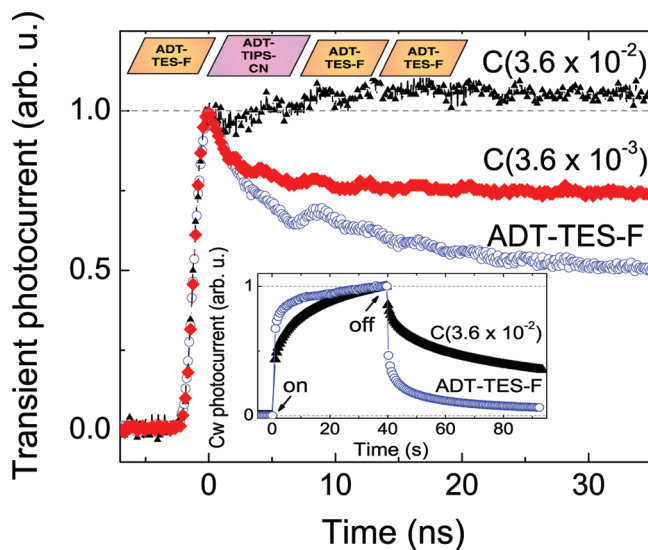


Figure 4. Transient photocurrents, normalized by their values at the peak at $t = 0$, obtained in pristine ADT-TES-F and ADT-TES-F/ADT-TIPS-CN ($C(3.6 \times 10^{-3})$ and $C(3.6 \times 10^{-2})$) films under 355 nm, 500 ps pulsed excitation. The inset shows photocurrents, normalized by their values at $t = 40$ s, measured in pristine ADT-TES-F and $C(3.6 \times 10^{-2})$ films under cw 532 nm excitation. At $t = 0$ s (40 s), the light is turned on (off).

which efficient exciplex formation was confirmed by the PL data, the peak amplitude at $t = 0$ was reduced by ~ 27 and 53%, respectively, which is in part due to changes in film morphology^{2,21,22,27} upon addition of the ADT-TIPS-CN and in part due to reduction in the density of charge carriers photogenerated at sub-500 ps time scales. In the $C(3.6 \times 10^{-3})$ sample, the photocurrent dynamics were similar to those in the pristine ADT-TES-F film at times below ~ 5 ns after excitation, after which a slower decay persisted, characterized by a power-law function with an exponent β of 0.032. In the $C(3.6 \times 10^{-2})$ sample, an additional slow component of charge photogeneration was observed, which resulted in an increase in photocurrent at nanosecond time scales, with a peak response occurring at ~ 20 ns after excitation. Photocurrents from pristine ADT-TIPS-CN films under similar conditions were at least 3 orders of magnitude lower than those from pristine ADT-TES-F films. Therefore, the contribution of dissociated ADT-TIPS-CN excitons, created either via direct excitation of ADT-TIPS-CN or via excitation of ADT-TES-F followed by FRET, to the photocurrent in ADT-TES-F/ADT-TIPS-CN composites is negligible. Thus, the most likely source of charge carriers contributing to charge photogeneration at nanosecond time scales is the dissociated ADT-TES-F/ADT-TIPS-CN exciplex. Similarity between the time scales of the slower component of the charge carrier photogeneration in the $C(3.6 \times 10^{-2})$ sample (Figure 4) and of the exciplex PL decay (Figure 3b) supports this conclusion. In the $C(3.6 \times 10^{-2})$ sample, the carriers originating from the exciplex contributed $\sim 5\%$ of the total transient photocurrent amplitude. At higher ADT-TIPS-CN concentrations, larger contributions from exciplex dissociation into the transient photocurrent were observed (e.g., $\sim 30\%$ in the $C(1.8 \times 10^{-1})$ sample in ref 2). At time scales above ~ 20 ns, a slow power-law photocurrent decay with $\beta = 0.026$ was measured in the $C(3.6 \times 10^{-2})$ sample. The drastic slowing down of the photocurrent decay upon addition of the ADT-TIPS-CN to the ADT-TES-F host is due to inhibited

charge carrier recombination in the composite samples. This occurs due to efficient trapping of the electron by the ADT-TIPS-CN, enabling the hole to freely propagate in the ADT-TES-F host. Similar trends in charge carrier dynamics were observed on the time scales of tens of seconds after photoexcitation²⁴ in the photocurrent measured under cw 532 nm illumination. In composites, reduced amplitudes of the steady-state photocurrent (e.g., by ~60% in the C(3.6×10^{-2}) sample) and significantly slower charge carrier recombination (inset of Figure 4) were obtained, as compared to the pristine ADT-TES-F film.

In summary, ADT-TES-F and ADT-TIPS-CN molecules embedded in a PMMA matrix form a D/A FRET pair with a Förster radius R_0 of 4.8 nm. In ADT-TES-F/ADT-TIPS-CN composite films, containing the bulk D/A heterojunctions, the dominant D/A interaction is exciplex formation. PL emission from the exciplex, peaked at ~668 nm, dominated PL spectra of the composites. Although the exciplex contributed to charge carrier photogeneration at nanosecond time scales, the overall effect of ADT-TIPS-CN addition to the ADT-TES-F host was detrimental to the photoresponse amplitude. Larger energy offsets between the donor and acceptor molecules would be necessary to improve charge photogeneration efficiency. However, significantly slower charge carrier recombination in ADT-TES-F/ADT-TIPS-CN composites, as compared to that in pristine ADT-TES-F films, could be beneficial for applications requiring effective storage of photogenerated charge carriers such as bistable optical switches, photodetectors, and image storage devices. By varying relative concentrations of the ADT-TES-F and ADT-TIPS-CN, desired photocurrent dynamics can be obtained.

■ ASSOCIATED CONTENT

S Supporting Information. Sample preparation, relations between guest concentration and average intermolecular spacings, experimental methods, FRET radius calculations, multipeak fitting example, and catalogue of PL spectral peaks for ADT-TES-F and ADT-TIPS-CN isolated and aggregated molecules and the exciplex. This material is available free of charge via the Internet at <http://pubs.acs.org>.

■ AUTHOR INFORMATION

Corresponding Author

*E-mail: oksana@science.oregonstate.edu.

■ ACKNOWLEDGMENT

This work was supported by the National Science Foundation via CAREER program (DMR-0748671) and the Office of Naval Research (N00014-05-1-0019). W.E.B.S. thanks the SPIE Educational Scholarship in Optical Science and Engineering for support.

■ REFERENCES

- (1) Katz, H.; Huang, J. Thin-Film Organic Electronic Devices. *Annu. Rev. Mater. Res.* **2009**, *39*, 71–92.
- (2) Day, J.; Platt, A. D.; Ostroverkhova, O.; Subramanian, S.; Anthony, J. E. Organic Semiconductor Composites: Influence of Additives on the Transient Photocurrent. *Appl. Phys. Lett.* **2009**, *94*, 013306.
- (3) Heeger, A. J. Semiconducting Polymers: The Third Generation. *Chem. Soc. Rev.* **2010**, *39*, 2354–2371.

- (4) Ostroverkhova, O.; Moerner, W. E. Organic Photorefractives: Mechanisms, Materials, and Applications. *Chem. Rev.* **2004**, *104*, 3267–3314.

- (5) Kim, Y.; Ballarotto, M.; Park, D.; Du, M.; Cao, W.; Lee, C. H.; Herman, W. N.; Romero, D. B. Interface Effects on the External Quantum Efficiency of Organic Bulk Heterojunction Photodetectors. *Appl. Phys. Lett.* **2007**, *91*, 193510.

- (6) Coffey, D. C.; Ferguson, A. J.; Kopidakis, N.; Rumbles, G. Photovoltaic Charge Generation in Organic Semiconductors Based on Long-Range Energy Transfer. *ACS Nano* **2010**, *4*, 5437–5445.

- (7) Baldo, M. A.; Thompson, M. E.; Forrest, S. R. High-Efficiency Fluorescent Organic Light-Emitting Devices Using a Phosphorescent Sensitizer. *Nature* **2000**, *403*, 750–753.

- (8) Poortmans, J.; Arkhipov, V., Eds. *Thin Film Solar Cells: Fabrication, Characterization and Applications*; Wiley: New York, 2006.

- (9) Weller, A. In *The Exciplex*; Gordon, M., Ware, W., Eds.; Academic: New York, 1975; pp 23–28.

- (10) Förster, T. In *The Exciplex*; Gordon, M., Ware, W., Eds.; Academic: New York, 1975; pp 1–21.

- (11) Offermans, T.; van Hal, P.; Meskers, S.; Koetse, M. Exciplex Dynamics in a Blend of π -Conjugated Polymers with Electron Donating and Accepting Properties: MDMO-PPV and PCNEPV. *Phys. Rev. B* **2005**, *72*, 45213.

- (12) Morteani, A.; Sreearunthai, P.; Herz, L.; Friend, R. Exciton Regeneration at Polymeric Semiconductor Heterojunctions. *Phys. Rev. Lett.* **2004**, *92*, 247402.

- (13) Rand, B. P.; Burk, D. P. Offset Energies at Organic Semiconductor Heterojunctions and their Influence on the Open-Circuit Voltage of Thin-Film Solar Cells. *Phys. Rev. B* **2007**, *75*, 115327.

- (14) Li, F.; Chen, Z.; Wei, W.; Cao, H.; Gong, Q.; Teng, F.; Qian, L.; Wang, Y. Blue-Light-Emitting Organic Electroluminescence via Exciplex Emission Based on a Fluorene Derivative. *J. Phys. D: Appl. Phys.* **2004**, *37*, 1613–1616.

- (15) Benson-Smith, J. J.; Wilson, J.; Dyer-Smith, C.; Mouri, K.; Yamaguchi, S.; Murata, H.; Nelson, J. Long-Lived Exciplex Formation and Delayed Exciton Emission in Bulk Heterojunction Blends of Silole Derivative and Polyfluorene Copolymer: The Role of Morphology on Exciplex Formation and Charge Separation. *J. Phys. Chem. B* **2009**, *113*, 7794–7799.

- (16) Yin, C.; Kietzke, T.; Neher, D.; Hörhold, H.-H. Photovoltaic Properties and Exciplex Emission of Polyphenylenevinylene-Based Blend Solar Cells. *Appl. Phys. Lett.* **2007**, *90*, 092117.

- (17) Palilis, L. C.; Mäkinen, A. J.; Uchida, M.; Kafafi, Z. H. Highly Efficient Molecular Organic Light-Emitting Diodes Based on Exciplex Emission. *Appl. Phys. Lett.* **2003**, *82*, 2209.

- (18) Morteani, A.; Dhoot, A.; Kim, J.-S.; Silva, C.; Greenham, N.; Murphy, C.; Moons, E.; Ciná, S.; Burroughes, J.; Friend, R. Barrier-Free Electron–Hole Capture in Polymer Blend Heterojunction Light-Emitting Diodes. *Adv. Mater.* **2003**, *15*, 1708–1712.

- (19) Anthony, J. E. Functionalized Acenes and Heteroacenes for Organic Electronics. *Chem. Rev.* **2006**, *106*, 5028–5048.

- (20) Park, S. K.; Mourey, D. A.; Subramanian, S.; Anthony, J. E.; Jackson, T. N. High-Mobility Spin-Cast Organic Thin Film Transistors. *Appl. Phys. Lett.* **2008**, *93*, 043301.

- (21) Day, J.; Subramanian, S.; Anthony, J. E.; Lu, Z.; Twieg, R. J.; Ostroverkhova, O. Photoconductivity in Organic Thin Films: From Picoseconds to Seconds After Excitation. *J. Appl. Phys.* **2008**, *103*, 123715.

- (22) Platt, A. D.; Day, J.; Subramanian, S.; Anthony, J. E.; Ostroverkhova, O. Optical, Fluorescent and (Photo)conductive Properties of High-Performance Functionalized Pentacene and Anthradithiophene Derivatives. *J. Phys. Chem. C* **2009**, *113*, 14006–14014.

- (23) Shepherd, W. E. B.; Platt, A. D.; Hofer, D.; Ostroverkhova, O.; Loth, M.; Anthony, J. E. Aggregate Formation and its Effect on (Opto)Electronic Properties of Guest–Host Organic Semiconductors. *Appl. Phys. Lett.* **2010**, *97*, 163303.

- (24) Shepherd, W. E. B.; Platt, A. D.; Banton, G.; Hofer, D.; Loth, M. A.; Anthony, J. E.; Ostroverkhova, O. Effect of Intermolecular

Interactions on Charge and Exciplex Formation in High-Performance Organic Semiconductors. *Proc. SPIE* **2011**, 7935.

(25) Lakowicz, J. R. *Principles of Fluorescence Spectroscopy*; Springer: New York, 2006.

(26) Dyer-Smith, C.; Benson-Smith, J. J.; Bradley, D. D. C.; Murata, H.; Mitchell, W. J.; Shaheen, S. E.; Haque, S. A.; Nelson, J. The Effect of Ionization Potential and Film Morphology on Exciplex Formation and Charge Generation in Blends of Polyfluorene Polymers and Silole Derivatives. *J. Phys. Chem. C* **2009**, *113*, 14533–14539.

(27) Ostroverkhova, O.; Shcherbina, S.; Cooke, D. G.; Egerton, R. F.; Hegmann, F. A.; Tykwinski, R. R.; Parkin, S. R.; Anthony, J. E. Optical and Transient Photoconductive Properties of Pentacene and Functionalized Pentacene Thin Films: Dependence on Film Morphology. *J. Appl. Phys.* **2005**, *98*, 033701.